Conference paper

Laura J.B.M. Kollau, Mark Vis*, Adriaan van den Bruinhorst, Gijsbertus de With and Remco Tuinier

Activity modelling of the solid–liquid equilibrium of deep eutectic solvents

https://doi.org/10.1515/pac-2018-1014

Abstract: Compared to conventional solvents used in the chemical industry, deep eutectic solvents (DESs) are considered as promising potentially sustainable solvents. DESs are binary mixtures and the resulting liquid mixture is characterized by a large melting point depression with respect to the melting temperatures of its constituents. The relative melting point depression becomes larger as the two components have stronger attractive interactions, resulting in non-ideal behavior. The compositional range over which such binary mixtures are liquids is set by the location of the solid–liquid phase boundary. Here we present experimental phase diagrams of various recent and new DESs that vary in the degree of non-ideality. We investigate whether thermodynamic models are able to describe the solid–liquid equilibria and focus on relating the parameters of these models to the non-ideal behavior, including asymmetric behavior of the activity coefficients. It is shown that the orthogonal Redlich–Kister-like polynomial (OP) expansion, including an additional first order term, provides an accurate description. This theory can be considered as an extension of regular solution theory and enables physical interpretation of the fit parameters.

Keywords: deep eutectic solvent; eutectic mixture; ISSP-18; phase behavior; solid–liquid coexistence; thermodynamic modelling.

Introduction

Deep eutectic solvents (DESs), introduced at the beginning of this century [1], are binary mixtures that have melting points significantly below those of the individual substances. Since a wide range of components can be selected as DES combinations, many resulting binary liquids may be compliant with the green chemistry

Article note: Part of a collection of invited papers based on presentations at the 18th International Symposium on Solubility Phenomena and Related Equilibrium Processes (ISSP-18), Tours, France, 15–20 July 2018.

***Corresponding author: Mark Vis,** Laboratory of Physical Chemistry, Department of Chemical Engineering and Chemistry, Eindhoven University of Technology, P.O. Box 513, 5600MB Eindhoven, The Netherlands; and Institute for Complex Molecular Systems, Eindhoven University of Technology, Eindhoven, The Netherlands, e-mail: m.vis@tue.nl. https://orcid.org/0000-0002-2992-1175
Laura J.B.M. Kollau: Laboratory of Physical Chemistry, Department of Chemical Engineering and Chemistry, Eindhoven University of Technology, P.O. Box 513, 5600MB Eindhoven, The Netherlands; and Institute for Complex Molecular Systems, Eindhoven University of Technology, Eindhoven, The Netherlands. https://orcid.org/0000-0003-3713-0637
Adriaan van den Bruinhorst and Gijsbertus de With: Laboratory of Physical Chemistry, Department of Chemical Engineering and Chemistry, Eindhoven University of Technology, P.O. Box 513, 5600MB Eindhoven, The Netherlands. https://orcid.org/0000-0002-7163-8429 (G. de With)
Remco Tuinier: Laboratory of Physical Chemistry, Department of Chemical Engineering and Chemistry, Eindhoven University of Technology, P.O. Box 513, 5600MB Eindhoven, The Netherlands; Institute for Complex Molecular Systems, Eindhoven University of Technology, Eindhoven, The Netherlands; and Van 't Hoff Laboratory for Physical and Colloid Chemistry, Debye Institute for Nanomaterials Science, Utrecht University, Utrecht, The Netherlands. https://orcid.org/0000-0002-4096-7107

principles [2]. The identification of new DESs is, however, often followed by directly focusing on possible applications [3–6] of the liquids, while the phase diagrams and other fundamental properties scarcely receive attention [7–11]. A key characteristic of DESs is the larger decrease in melting point upon mixing the constituents, which is maximal at the eutectic composition and is significantly stronger as compared to ideal melting point depression. However, there is no consensus yet on how large the decrease in melting point should be, or what the reference should be in order to refer to a particular eutectic mixture as a deep eutectic solvent. Recently research into the nature of the interactions responsible for this non-ideal behavior has emerged [12–18]. Work on the prediction of solid–liquid phase behavior has been performed with PC-SAFT [19, 20], although the interpretation of such models is not completely straightforward. Previously, we applied regular solution (RS) theory to eutectic phase behavior to quantify the non-ideal interactions between the components with a single parameter [21]. The advantage of RS theory is that it yields an interaction parameter which is independent of composition and has a physical meaning [20, 22]. However, RS theory is limited to describing systems that exhibit symmetric non-ideal behavior and, as shown here, moderate non-idealities only.

Here we explore to which degree thermodynamic models are able to quantify and describe the solid–liquid equilibrium behavior of recently reported [21] and well-defined eutectic mixtures, frequently called deep eutectic solvents. We compare a commonly used engineering model, non-random two-liquid theory (NRTL) [23–26], to describe two-phase equilibria, and study the accuracy of using the Redlich–Kister approach [27, 28]. Particularly, we use a systematic orthogonal Redlich–Kister-like polynomial (OP) expansion [29, 30], which can be considered as originating from RS theory. We quantitatively compare the models using a variance analysis to assess the significance of each additional parameter. Since these models yield multiple interaction parameters, we calculate the corresponding activity coefficients to express the non-ideality. In order to evaluate the suitability of these models to describe the solid–liquid equilibrium for a range of non-idealities in DESs, we studied three binary mixtures which differ in one component and in non-ideality. This enables to assess the suitability of these models to describe different degrees of non-ideality featured by eutectic mixtures.

Figure 1 presents the components used to measure the phase diagrams; erythritol (E), succinic acid (S), pimelic acid (P) and Pe_4NBr (T). The DESs composed of these components are denoted as ET, ST and PT. These systems represent a mildly non-ideal DES (ET), a moderately non-ideal DES (ST), and a strongly non-ideal DES (PT).

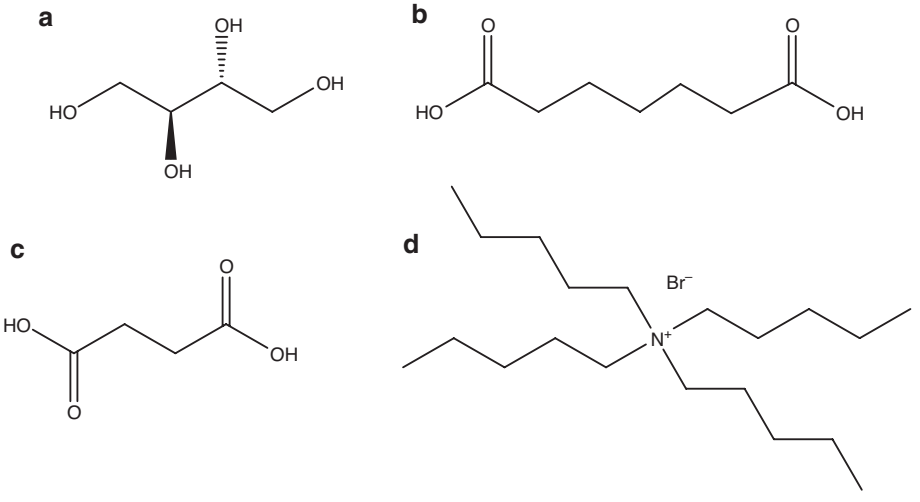

Fig. 1: Chemical structures of the components used for the DESs studied: (a) erythritol, (b) pimelic acid, (c) succinic acid, and (d) Pe_4NBr.

Materials and methods

Characterization of the individual components

The chemicals used to prepare the DESs are listed in Table 1. The chemicals were dried overnight under vacuum before use. The water content of the individual components was measured using a Metrohm 831 KF coulometer with a generator electrode with diaphragm and Hydranal Coulomat AG was used as titration medium. The detection limit is 10 µg. Samples of approximately 1.5 g were heated until fully melted using an 832 KF Thermoprep to measure all water present. The melting points and enthalpies of fusion measured are listed in Table 2 and compared to literature values. The melting points measured are within 1 % of the literature values. The enthalpies of fusion of the dicarboxylic acids are higher than found in literature, erythritol is comparable, and Pe_4NBr is slightly lower. The measurements were performed using a TA Q2000 Dynamic Scanning Calorimeter (DSC), with an accuracy of ±0.1 K for T^* and <1 % for ΔH, and a precision for T^* of ±0.4 K. The melting point was determined from the minimum of the temperature derivative of the heat flow at the descent of the melting peak at a heating rate of 1 K · min^{-1}.

DES preparation and characterization

Glass containers, spatulas and tweezers were dried overnight in an oven at 105 °C. The dried utensils were transferred into a glovebox with inert nitrogen atmosphere with typical values of 0.5 ppm O_2 and 1.5 ppm H_2O. The overpressure in the glovebox was kept at 1.5–2.5 mbar. The mass of the individual components of the DESs was determined inside the glovebox using weighing boats and an analytical balance, with a resolution of 0.1 mg. Together with a magnetic stirring bar, the components were added to a glass vial. Subsequently the mixture was heated above the highest melting point (T^*) of the individual components while stirring. The resulting liquid mixture was poured in a mortar, cooled down, and after crystallization grounded with a pestle to obtain homogenous, fine powders. Samples were prepared covering a wide composition range.

Table 1: Characteristics of the individual components from which the DESs studied were prepared.

Name	CAS	Grade	Water content [ppm]	T^* [K]		ΔH [kJ · mol^{-1}]	
				(Meas.)	([a]Lit.)	(Meas.)	([a]Lit.)
Succinic acid	110-15-6	>99 %	6.1	460.0	461.0 [31]	37.10	34.00 [32]
Erythritol	149-32-6	>99 %	7.7	394.7	392.2 [33]	39.30	39.40 [34]
Pimelic acid	111-16-0	98 %	7.7	378.5	379.2 [31]	26.07	23.70 [32]
Pe_4NBr	866-97-7	>99 %	7.3	375.9	373.2 [35–38]	40.14	41.45 [39]

Melting point T^* and enthalpy of fusion ΔH for the components used. [a]References indicated in square brackets.

Table 2: Expressions for the Gibss excess molar energy ΔG^E of various polynomial expansions of RS theory.

Model	Abbreviation	$\Delta G^E/RT$	Equation number
Regular solution theory	RS	$x_1x_2\chi$	1
Redlich–Kister	RK	$x_1x_2[k_0+k_1(x_1-x_2)+k_2(x_1-x_2)^2+\cdots]$	2
Orthogonal Redlich–Kister-like polynomial	OP	$x_1x_2\left[p_0+p_1Z+p_2\frac{1}{2}(3Z^2-1)+\cdots\right]$	3a
		$Z=x_1-x_2=2x_1-1$	3b

A capillary melting point apparatus (Büchi melting point B-540) was used to measure the melting points and eutectic temperatures of the DESs ET and ST. For each composition two capillaries were filled with approximately 5.0 mm of fine sample powders and hermetically closed with hot glue before removal from the glovebox. The samples were first heated at a rate of 5 $K \cdot min^{-1}$ and the eutectic temperature was recorded when the first liquid appeared. Next, the samples were cooled to RT and crystallized for at least 24 h. Subsequently, the samples were heated at 1 $K \cdot min^{-1}$ until a uniform liquid was obtained. The eutectic temperature (solidus) was recorded upon the first appearance of liquid and the melting point (liquidus) upon the disappearance of the last amount of solid. After complete liquefaction and subsequent crystallization, the first melt could not be readily distinguished from the neatly recrystallized phase. Therefore, only the melting point was determined in the last heating step at 1 $K \cdot min^{-1}$, yielding two solidus and liquidus temperatures in total. For a given composition, this was executed using at least two samples. During all heating cycles, images of the mixtures were recorded using a photo camera (Canon EOS 50D, Macro Lens EF 100 mm 1:2.8 USM), capturing a photo every 5 s.

The measurements of the eutectic temperature of PT was performed as for ET and ST, while the melting points were measured using a TA Q2000 DSC, because kinetic effects disturbed the capillary melting method. Two samples of each composition were cramped into Tzero hermetic aluminum pans inside the glovebox. These samples were measured using four heating–cooling cycles. During the first and second cycle the sample was heated at 10 $K \cdot min^{-1}$ to 10 K above the melting point of highest melting component. Cooling was performed at a rate of 10 $K \cdot min^{-1}$ until 263 K. Subsequently, the sample was heated again to 288 K and held isothermally for 5 min to allow complete recrystallization. This sequence was the same for all cycles. For the third and fourth heating cycle the applied heating rate was 5 $K \cdot min^{-1}$ and 1 $K \cdot min^{-1}$, respectively. The apparent melting points were determined at all three heating rates by taking the minimum of the temperature derivative of the heat flow at the descent of the last peak. The melting point was determined by extrapolating the apparent melting points to a heating rate of 0 $K \cdot min^{-1}$.

The composition of the mixture in each melting point capillary and DSC sample was determined by ^{1}H-NMR spectroscopy (Bruker BZH 400/52) after the measurements. D_2O (Cambridge Isotope Laboratories Inc. Deuterium oxide 99.9 %, DLM-4-100, CAS 7789-20-0) was used as solvent.

Theory

Deviations from ideal behavior can be quantified straightforwardly by activity coefficients. Classically, activity coefficients are a common manner to link activities to concentrations and for a binary mixture composed of components $i = 1, 2$ they are related to the molar Gibbs mixing energy $\Delta_{mix}G$, the ideal Gibbs energy ΔG^{id} and the Gibbs excess energy ΔG^{E} [40] as follows:

$$\Delta_{mix}G = \Delta G^{id} + \Delta G^{E} \tag{4}$$

$$RT \ln \gamma_i = \frac{\partial (n \Delta G^{E})}{\partial n_i} \tag{5}$$

Note that we use molar Gibbs energies throughout. The activity coefficient γ_i is related to $\Delta\mu_i$ via:

$$\ln \gamma_i x_i = \frac{\Delta \mu_i}{RT} = -\frac{\Delta H_i}{R}\left(\frac{1}{T} - \frac{1}{T_i^*}\right) \tag{6}$$

where T is the melting point of the mixture and T_i^* the melting point of the individual component. For simplicity we assume the enthalpy independent of temperature, thus assuming a constant heat capacity. The molar excess Gibbs energy ΔG^{E} is then obtained after subtracting ΔG^{id}, which is obtained when $\gamma_i = 1$. The studied solid–liquid phase diagrams were obtained by measuring the eutectic temperature and

melting points for various compositions as described in Section "Materials and methods". For each activity coefficient model explored here (see Table 2), this generates an expression to describe the solid–liquid equilibrium with certain fit parameters.

OP expansion

Regular solution (RS) theory was proposed by Hildebrand and Scott [41] and is originally based on a lattice model with random mixing of components 1 and 2 in case of binary mixture. The entropy of mixing in this model is considered to be ideal, so $S^E = 0$ and $H^E = G^E$. The non-ideality results from short-ranged nearest neighbor interactions of component 1 with component 2 according to eq. 1 in Table 2. The excess functions can be expanded in a Taylor series and the resulting coefficients can be interpreted as interaction parameters. This is especially helpful when considering systems at higher concentrations, at which the partial molar properties are non-linear functions of composition. Redlich and Kister [27, 28] proposed such an expansion by adding a polynomial in $(x_1 - x_2)$. The RK polynomial (eq. 2 in Table 2) has the advantage that corrections on the result are imposed from the center $x_1 = x_2 = 0.5$ towards lower and higher mole fractions. Pelton and Bale [29] used an *orthogonal* polynomial in $(x_1 - x_2)$, (eq. 3 in Table 2). The OPs are essentially Legendre polynomials in $(x_1 - x_2)$ with the property that the various coefficients are independent of each other. This allows the evaluation the significance of every added coefficient (fit parameter) separately. The zeroth order terms in RS theory and the OP expansion are identical, $\chi = p_0$, and thus can still considered to be a property of the binary mixture. Here we compare the RS fits resulting from fitting to solidus data only [21], with the results from the OP expression for the p_0 parameter fitted to all the data available, thus also including the liquidus data. The variance, however, will be determined from the liquidus and solidus data for both methods.

NRTL

The non-random two-liquid (NRTL) model is one of the most well-known local composition models for thermodynamic excess functions. The detailed expressions for the activity coefficients for this model can be found in the supplementary information (SI). These expressions basically are an extension of Wilson's equations [42], including a non-randomness parameter [43] α. The non-randomness arises from the difference in interaction energy of the central molecule with the molecules of its own kind, and that with molecules of the other kind. It is noted that the assumption made in both the Wilson and the original NRTL equations (with α taken as a constant) that the local compositions around the central molecules *i* and *j* are independent of each other leads to an inconsistency in the overall composition of the mixture [44, 45].

Results and discussion

Figure 2 (left panel) show the obtained phase diagrams for the chosen DESs. The data points shown result from averages of the raw data provided in the SI. The error bars depicted are the resulting standard deviations after grouping data points for clarity. The fits were performed on the raw data. The first observation of the figures is the clear deviation between the measured data points and predicted ideal behavior (gray curves). The non-ideality can be quantified directly from the solidus data (eutectic temperature) using RS theory which allows for a subsequent prediction of the full phase diagram, which are the blue dashed curves in Fig. 2. This results in a reasonable description of the phase diagram for ET and ST. For PT only a qualitative description of the phase behavior is achieved. We expect that these quantitative discrepancies become larger with stronger non-idealities.

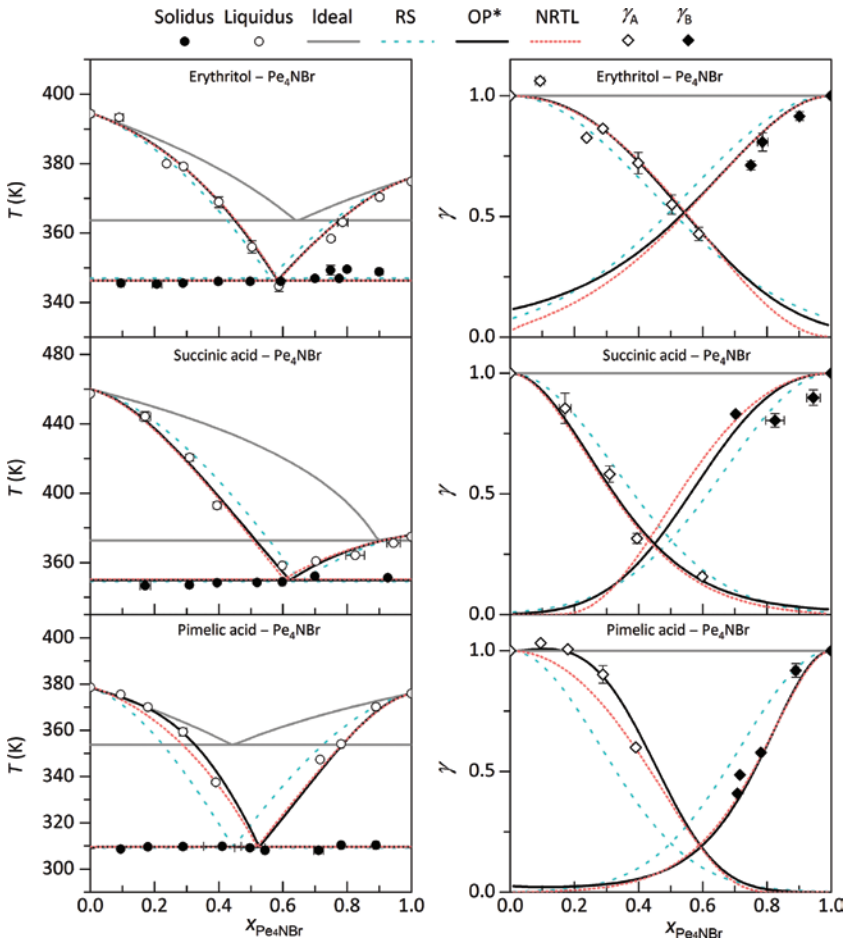

Fig. 2: Left: Obtained phase diagrams of the indicated DESs, Pe_4NBr with erythritol (ET), succinic acid (ST) and pimelic acid (PT), together with the fit resulting from the different models. Right: Activity coefficients γ_A of either erythritol, succinic acid or pimelic acid respectively, and γ_B of Pe_4NBr, together with the calculated activity coefficients resulting from the different models for each DES. OP* is the best fitting orthogonal polynomial expansion, which in case of ET is zeroth order, ST and PT first order.

A characteristic of RS theory is that with a more negative interaction parameter χ (i.e. stronger effective attractions), the eutectic point limits to $x_1 = x_2 = 0.5$. Therefore, the eutectic composition cannot be shifted beyond this point when varying χ and this has important implications. In the case of PT, the 'ideal' eutectic point is situated at $x_{Pe_4NBr} < 0.5$, while the experimental data suggests that the eutectic point lies at $x_{Pe_4NBr} > 0.5$. This characteristic means that RS theory cannot describe this phase behavior accurately. To account for the experimentally detected asymmetric non-ideality, we evaluated models with additional degrees of freedom. For this we used the orthogonal Redlich–Kister-like polynomial (OP) and used the NRTL model as a benchmark. The value of every additional order was evaluated using an *F*-test. This revealed that for ET the expansion does not add value, which is expected since the discrepancy between the fit and data is comparable to the experimental accuracy (±0.5 K). For ST and PT the addition of a first order term improves the fit significantly, as the difference in standard error is significantly larger than the experimental accuracy. The OP expansion was truncated after the first order term, since adding higher orders did not result in a statistically better fit.

The first order OP descriptions perform equally well or better than the benchmark NRTL model, while the OP model has only two fit parameters. The parameter p_0 is directly related to the eutectic temperature and p_1 is related to the asymmetry of the phase diagram. The models fitted to the temperature data also accurately describe the non-ideality as expressed by the activity coefficients, see Fig. 2 (right panel). Table 3

Table 3: Summary of the obtained eutectic composition (mole fractions) and temperature for all the models and DESs: Pe_4NBr with erythritol (ET), succinic acid (ST) and pimelic acid (PT).

Model		ET		ST		PT	
		x_{eut}	T_{eut} [K]	x_{eut}	T_{eut} [K]	x_{eut}	T_{eut} [K]
Ideal		0.67	364.1	0.90	372.9	0.44	353.8
RS	Solidus	0.56	347.0	0.66	349.3	0.45	309.3
OP	$n=0$	0.57	347.7	0.65	346.6	0.45	310.7
	$n=1$	0.59	346.4	0.62	350.0	0.53	309.6
	$n=2$	0.59	346.5	0.62	350.0	0.52	309.4
NRTL	$\alpha=0.3$	0.59	346.3	0.61	350.4	0.52	309.6

Table 4: Overview of the fit parameters, *a*, *b* and *c*, of all models for all DESs: Pe_4NBr with erythritol (ET), succinic acid (ST) and pimelic acid (PT).

Model		ET				ST				PT			
		a	*b*	*c*	SE [K]	*a*	*b*	*c*	SE [K]	*a*	*b*	*c*	SE [K]
Ideal					13.2				27.1				37.8
RS	Solidus	−2.59			2.26	−4.68			5.53	−6.37			5.55
OP	$n=0$	−2.61			2.49	−5.14			4.91	−6.22			5.50
	$n=1$	−2.63	−0.46		1.94	−4.85	1.03		3.35	−6.44	−2.33		1.44
	$n=2$	−2.72	−0.49	−0.28	1.82	−4.88	1.02	−0.56	3.32	−6.29	−2.19	0.37	1.18
NRTL	$\alpha=0.3$	−1567.0	−4735.4		2.04	−8862.0	−1565.7		3.67	−2578.1	−9125.3		2.3

For RS theory parameter *a* represents χ. For OP of order *n*, *a, b* and *c* represent p_0, p_1 and p_2. For NRTL *a* represents g_{12} and *b* represents g_{21} (in $J \cdot mol^{-1}$). SE is the standard error between the fit and the data points.

Table 5: Variance analysis summary for the different models used to fit the DESs: Pe_4NBr with erythritol (ET), succinic acid (ST) and pimelic acid (PT).

Model 1	Model 2	ET	ST	PT
		$F_c=1.48$	$F_c=1.64$	$F_c=1.60$
RS	OP	1.36	2.73	14.8
RS	NRTL	1.20	2.27	10.6
NRTL	OP	1.11	1.20	1.82

The critical *F*-value (F_c) was determined at a significance level of $\alpha=0.05$.

summarizes the obtained eutectic point and eutectic temperature for every model applied. Table 4 presents an overview of all the fit parameters for the different models and in Table 5 a summary of the variance analysis is listed. For the full variance analysis data, see the ESI. Finally, we note that we used mole fractions as is commonly done; however, in view of the size difference between the molecules of the different components it may be more appropriate to use volume fractions instead. The present model considers an excess free energy in which we do not explicitly distinguish entropic and enthalpic interactions. A natural follow-up is to include excess entropy of mixing in a theoretical framework such as Flory–Huggins entropy of mixing or Guggenheim–Staverman entropy of mixing. The authors refer the interested readers to work in which the Flory–Huggins entropy of mixing is applied to these eutectic mixtures [46]. The interaction parameter χ decreases if Flory–Huggins mixing entropy is accounted for, which is enhanced whenever the molar volumes of the components differ more.

Conclusions

We studied the phase behavior of binary mixtures that exhibit non-ideal eutectic behavior. The liquid regions of such mixtures are often termed deep eutectic solvents (DESs). We focused on using various thermodynamic models to quantitatively describe the solid–liquid equilibrium. We present recently reported phase diagrams of DESs plus a phase diagram of a new DES which exhibits strongly non-ideal behavior. We showed that regular solution theory provides a measure for the non-ideality of DESs, also when strong attractions are present. In case of strongly non-ideal behavior, it is necessary to take the asymmetry of the non-ideality into account in order to quantitatively describe the liquidus data and to make an accurate interpolation of the eutectic point. To this purpose we used Redlich–Kister-like orthogonal polynomial (OPs) as an expansion for RS theory and compared the results with the NRTL model. We showed that OPs yield a description at least as good as NRTL, while having only two fit parameters. The addition of a second or higher order terms in the OP expansion did not result in a significantly better description of the solid–liquid equilibrium. Because the polynomial used is orthogonal the physical interpretation of the first OP parameter can be identified as the interaction parameter χ from RS theory, whereas the second parameter describes the asymmetry. The interaction parameter χ enables one to directly assess the extent of the non-ideality of any, simple, eutectic mixture.

Acknowledgment: We would like to thank ing. M.M.R.M. Hendrix, ing. E. van de Nieuwenhuizen and ing. J. Verhaak for providing experimental support, dr. A.C.C. Esteves and dr. J. van Spronsen for useful discussions, and the members of the ISPT "Deep Eutectic Solvents in the pulp and paper industry" consortium for their financial and in kind contribution. This consortium consists of the following organisations: Altri – Celbi, Buckman, Crown Van Gelder, CTP, DS Smith Paper, ESKA, Essity, Holmen, ISPT, Mayr-Melnhof Eerbeek, Metsä Fibre, Mid Sweden University, Mondi, Omya, Parenco BV, The Navigator Company, Sappi, Smurfit Kappa, Stora Enso, Eindhoven University of Technology, University of Aveiro, University of Twente, UPM, Valmet Technologies Oy, Voith Paper, VTT Technical Research Centre of Finland Ltd, WEPA and Zellstoff Pöls. Furthermore, this project received funding from the Bio-Based Industries Joint Undertaking under the European Union's Horizon 2020 research and innovation programme, Funder Id: http://dx.doi.org/10.13039/100010661, under grant agreement Provides no. 668970. MV acknowledges the Netherlands Organisation for Scientific Research (NWO) for a Veni grant (Funder Id: http://dx.doi.org/10.13039/501100003246, no. 722.017.005).

References

[1] A. P. Abbott, G. Capper, D. L. Davies, R. K. Rasheed, V. Tambyrajah. *Chem. Commun.* **1**, 70 (2003).
[2] P. T. Anastas, J. C. Warner. *Green Chemistry: Theory and Practice*. Oxford University Press, New York (1998).
[3] N. R. Rodriguez, P. F. Requejo, M. C. Kroon. *Ind. Eng. Chem. Res.* **54**, 11404 (2015).
[4] D. J. G. P. van Osch, L. F. Zubeir, A. van den Bruinhorst, M. A. A. Rocha, M. C. Kroon. *Green Chem.* **17**, 4518 (2015).
[5] L. Brinchi, F. Cotana, E. Fortunati, J. M. Kenny. *Carbohydr. Polym.* **94**, 154 (2013).
[6] A. Marcilla, A. Gómez-Siurana, C. Gomis, E. Chápuli, M. C. Catalá, F. J. Valdés. *Thermochim. Acta* **484**, 41 (2009).
[7] J. D. Mota-Morales, M. C. Gutiérrez, M. L. Ferrer, I. C. Sanchez, E. A. Elizalde-Peña, J. A. Pojman, F. Del Monte, G. Luna-Bárcenas. *J. Polym. Sci. Part A Polym. Chem.* **51**, 1767 (2013).
[8] H. G. Liao, Y. X. Jiang, Z. Y. Zhou, S. P. Chen, S. G. Sun. *Angew. Chemie Int. Ed.* **47**, 9100 (2008).
[9] Q. Zhang, K. De Oliveira Vigier, S. Royer, F. Jérôme. *Chem. Soc. Rev.* **41**, 7108 (2012).
[10] L. Moura, T. Moufawad, M. Ferreira, H. Bricout, S. Tilloy, E. Monflier, M. F. Costa Gomes, D. Landy, S. Fourmentin. *Environ. Chem. Lett.* **15**, 747 (2017).
[11] C. Florindo, L. C. Branco, I. M. Marrucho. *Fluid Phase Equilib.* **448**, 135 (2017).
[12] X. Meng, K. Ballerat-Busserolles, P. Husson, J.-M. Andanson. *New J. Chem.* **40**, 4492 (2016).
[13] H. Sun, Y. Li, X. Wu, G. Li. *J. Mol. Model.* **19**, 2433 (2013).
[14] O. S. Hammond, D. T. Bowron, K. J. Edler. *Angew. Chemie Int. Ed.* **56**, 9782 (2017).
[15] O. S. Hammond, D. T. Bowron, K. J. Edler. *Green Chem.* **18**, 2736 (2016).
[16] G. García, M. Atilhan, S. Aparicio. *Chem. Phys. Lett.* **634**, 151 (2015).
[17] C. Florindo, L. Romero, I. Rintoul, L. C. Branco, I. M. Marrucho. *ACS Sustain. Chem. Eng.* **6**, 3888 (2018).

[18] C. Florindo, A. J. S. McIntosh, T. Welton, L. C. Branco, I. M. Marrucho. *Phys. Chem. Chem. Phys.* **20**, 206 (2017).
[19] E. A. Crespo, L. P. Silva, M. A. R. Martins, M. Bülow, O. Ferreira, G. Sadowski, C. Held, S. P. Pinho, J. A. P. Coutinho. *Ind. Eng. Chem. Res.* **57**, 11195 (2018).
[20] P. V. A. Pontes, E. A.Crespo, M. A. R. Martins, L. P. Silva, C. M. S. S. Neves, G. J. Maximo, M. D. Hubinger, E. A. C. Batista, S. P. Pinho, J. A. P. Coutinho, G. Sadowski, C. Held. *Fluid Phase Equilib.* **448**, 69 (2017).
[21] L. J. B. M. Kollau, M. Vis, A. van den Bruinhorst, A. C. C. Esteves, R. Tuinier. *Chem. Commun.* **54**, 13351 (2018).
[22] M. A. R. Martins, S. P. Pinho, J. A. P. Coutinho. *J. Solution Chem.* (2018). DOI: 10.1007/s10953-018-0793-1.
[23] I. Díaz, M. Rodríguez, E. J. González, M. González-Miquel. *Chem. Eng. Sci.* **193**, 370 (2019).
[24] Z. Bouzina, M. R. Mahi, I. Mokbel, A. Negadi, C. Goutaudier, J. Jose, L. Negadi. *J. Chem. Thermodyn.* **128**, 251 (2019).
[25] C. Du, R. Dong, B. Qiao, Z. Jin, T. Ye, Yi. Zhang, M. Wang. *J. Chem. Thermodyn.* **128**, 1 (2019).
[26] H. Renon, J. M. Prausnitz. *AIChE J.* **14**, 116 (1968).
[27] O. Redlich, A. T. Kister. *J. Chem. Phys.* **15**, 849 (1947).
[28] O. Redlich, A. T. Kister. *Ind. Eng. Chem.* **40**, 341 (1948).
[29] A. D. Pelton, C. W. Bale. *Metall. Trans. A* **17**, 1057 (1986).
[30] C. J. Van Tyne, P. M. Novotny, S. K. Tarby. *Metall. Trans. B* **7**, 299 (1976).
[31] V. R. Thalladi, M. Nüsse, R. Boese. *J. Am. Chem. Soc.* **122**, 9227 (2000).
[32] M. V. Roux, M. Temprado, J. S. Chickos. *J. Chem. Thermodyn.* **37**, 941 (2005).
[33] H. Suzuki, H. Sunada. *Chem. Pharm. Bull.* **45**, 1688 (1997).
[34] G. Barone, G. Della Gatta, D. Ferro, V. Piacente. *J. Chem. Soc. Faraday Trans.* **86**, 75 (1990).
[35] H. Nakayama. *Bull. Chem. Soc. Jpn*. **54**, 3717 (1981).
[36] M. J. McDowell, C. A. Kraus. *J. Am. Chem. Soc.* **73**, 3293 (1951).
[37] H. M. Daggett, E. J. Bair, C. A. Kraus. *J. Am. Chem. Soc.* **73**, 799 (1951).
[38] J. C. Goodrich, F. M. Goyan, E. E. Morse, R. G. Preston, M. B. Young. *J. Am. Chem. Soc.* **72**, 4411 (1950).
[39] T. G. Coker, J. Ambrose, G. J. Janz. *J. Am. Chem. Soc.* **92**, 5293 (1970).
[40] G. de With. *Liquid-State Physical Chemistry*, 1st ed., Wiley-VCH, Weinheim (2013).
[41] J. H. Hildebrand, R. L. Scott. *The Solubility of Non-Electrolytes*, 3rd ed., Rheinhold, New York (1949).
[42] G. M. Wilson. *J. Am. Chem. Soc.* **86**, 127 (1964).
[43] R. L. Scott. *J. Chem. Phys.* **25**, 193 (1956).
[44] V. Flemr. *Collect. Czechoslov. Chem. Commun.* **41**, 3347 (1976).
[45] C. McDermott, N. Ashton. *Fluid Phase Equilib.* **1**, 33 (1977).
[46] L. J. B. M. Kollau. Eindhoven University of Technology (2019), PhD thesis, ISBN: 978-90-386-4750-0.

Supplementary Material: The online version of this article offers supplementary material (https://doi.org/10.1515/pac-2018-1014).